The specific activity (number of millimicromoles of *N*-methyl serotonin formed per milligram of protein in 90 minutes) of the supernatant fraction of whole-brain homogenate was 0.26. The enzyme from supernatant was purified by ammonium sulfate precipitation, with the highest specific activity (0.87) being found in the protein precipitated in the 45 to 55 percent ammonium sulfate fraction. This fraction was further purified on Sephadex G-100 equilibrated with 0.05*M* phosphate buffer (*p*H 7.5) with an approximate tenfold overall purification (specific activity, 2.54). Enzyme activity was linear with 5HT concentration (0 to 2.0 μmole). Boiled enzyme was inactive. The enzyme was localized in the subcellular fraction after discontinuous sucrose-gradient centrifugation as follows (*2*). Two 12-ml sucrose layers (1.2 and 0.8*M*) were overlain with 12 ml of whole-brain homogenate in 0.32*M* sucrose and centrifuged at 100,000*g* for 90 minutes. Three-milliliter fractions were collected and assayed for enzyme activity (Fig. 1). Peaks of enzyme activity were seen in the supernatant and "synaptosomal" areas.

The substrates included 5-hydroxytryptamine, tryptamine, *N*-methyltryptamine, 5-methoxytryptamine, 5-hydroxy-*N*,*N*-methyltryptamine, and norepinephrine. A portion (10 μg) of the enzyme purified on the Sephadex column was incubated with 5 μmole of the various substrates in 0.5 ml of incubation mixture, the optimum concentration of substrate, as shown with 5HT. Relative enzyme specificity was highest for this substance. The relative activity of this methyl transferase for various substrates is represented in Table 1. Under these reaction conditions, this enzyme is specific for methylating the amine nitrogen of indole(ethyl)amine substrate rather than the oxygen in the 5-position. Radioactive bufotenine, *N*-methyltryptamine and dimethyltryptamine chromatographed (thin layer) with known compounds on cellulose in isopropanol, ammonia, water (200:10:20); in 20 percent KCl in water; and in methanol, butanol, benzene, water (40:30:20:10).

We earlier attempted to explain the observed reversal of sedation by indoleamino acid after preliminary treatment with a monoamine oxidase inhibitor as being a result of the increased conversion of ^{14}C-5-hydroxytryptophan to bufotenine in the chick (*3*). The presence in brain of an indole(ethyl)amine *N*-methyltransferase that can convert indoleamines to centrally active *N*-methyl derivatives may account for this reversal. If such an enzyme is present in human brain, it might help explain Glassman's (*4*) evidence demonstrating the potentiation of the antidepressant effects of monoamine oxidase inhibitors with tryptophan loads. The presence of such an enzyme might also explain the mechanism of action of the monoamine oxidase inhibitors. In addition, this may account for the occasional psychotic reactions seen clinically after patients are treated with a monoamine oxidase inhibitor, or with amphetamines in doses high enough to result in monoamine oxidase inhibition (*5*).

We have recently demonstrated the presence of this enzyme in the brain of rat, with the highest specific activity in the brain stem and the lowest in cortical areas. In addition, we have evidence of the presence of this enzyme in infant parietal and adult frontal cortical tissue taken incidentally from man during neurosurgical procedures.

MERRILY MORGAN
ARNOLD J. MANDELL
Department of Psychiatry, University of California, San Diego, La Jolla 92037

References and Notes

1. J. Axelrod, in *Transmethylation and Methionine Biosynthesis*, S. K. Shapior and F. Schlenk, Eds. (Univ. of Chicago Press, Chicago, 1965).
2. S. H. Snyder, J. Glowinski, J. Axelrod, *Life Sci.* **4**, 797 (1965).
3. C. E. Spooner, A. J. Mandell, D. Brunet, M. Cruickshank, I. M. Sabbot, *Fed. Proc.* **27**, 540 (1968); A. J. Mandell and C. E. Spooner, in *Schizophrenia, An Appraisal*, D. V. S. Sankar, Ed. (Pergamon, New York, 1969).
4. A. Glassman, paper read at annual meeting of the Psychiatric Research Society, Mental Health Center, New Haven, Conn., 5 December 1968.
5. L. L. Iversen, J. Axelrod, J. Glowinski, in *Neuropsychopharmacology*, H. Brill, J. O. Cole, P. Deniker, H. Hippius, P. B. Bradley, Eds. (Excerpta Medica Foundation, New York, 1967).
6. Supported by NIMH grant MH-14360-02. We thank J. Biel of Aldrich Chemical Co. for supplying substrates and carrier indoles.

28 April 1969

2-p-Toluidinyl-6-Naphthalene Sulfonate: Relation of Structure to Fluorescence Properties in Different Media

Abstract. *Hydrated and anhydrous crystals of 2-p-toluidinyl-6-naphthalene sulfonate exhibit fluorescence spectra similar to those obtained for 2-p-toluidinyl-6-naphthalene sulfonate in water and in organic solvents, respectively. The molecular structure of anhydrous 2-p-toluidinyl-6-naphthalene sulfonate suggests extended electron resonance over the whole molecule and this is one of the causes of the spectral differences.*

The fluorescence properties of 2-*p*-toluidinyl-6-naphthalene sulfonate (TNS) are dependent upon the polarity and steric structure of the environment (*1*). It is practically nonfluorescent in water but fluoresces with different quantum yields when dissolved in organic solvents and when noncovalently bound to different native proteins (*2*). This property makes TNS useful as a probe for determining polarity of protein active sites and as a fluorescent monitor of substrate binding and enzyme activation processes which entail protein conformational changes (*3*, *4*). The variation of fluorescence characteristics with environment is not well understood and we have undertaken structural studies of TNS to provide more data on this problem.

Crystallization was effected by slow diffusion of water into a solution of TNS potassium salt dissolved in *N*,*N*-dimethylformamide. Two types of crystals (A and B) were obtained. Type A contains water in the crystal lattice, and upon removal from solution type A loses the water and changes to lattice type B; in the process the crystals crack

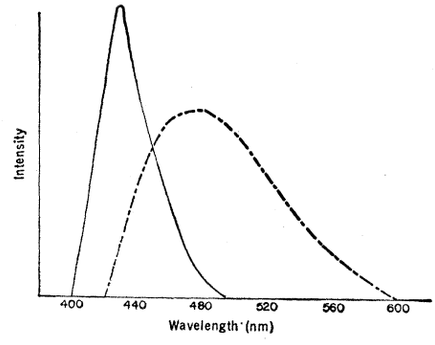

Fig. 1. Fluorescence spectra of TNS crystals. Solid line indicates anhydrous crystals; broken line indicates hydrated crystals.

and are destroyed. Good crystals of type B can be obtained by very slow evaporation of the same solution over a period of time. Cell constants are given in Table 1.

Crystals of both types were sealed in capillaries, the hydrated ones surrounded by mother liquid, and their emission spectra measured after excitation at 360 nm (Fig. 1). The fluorescence intensities of the two spectra are not quantitative relative to each other but peak shapes are accurate. The spectrum of anhydrous TNS crystals (type B) resembles very closely the TNS fluorescence spectrum in ethyl alcohol and other organic solvents, while that of the hydrated or type A crystals is similar to the TNS spectrum in water [see (*2*), p. 1913]. These similarities indicate that solvent-solute structural interactions are a likely cause of TNS fluorescence differences in different solvent environments. We show here the crystal and molecular structure of the anhydrous B crystal and present the structural information.

A full set of three-dimensional intensities was collected with MoKα on a four-circle diffractometer equipped with a scintillation counter. Over 2500 reflections were measured. The crystal structure was solved by interpretation of the three-dimensional Patterson function for the K, S, three O, and one C atom positions and subsequent location of all other atoms by successive Fourier syntheses. Refinement proceeded by least-squares adjustment of atom coordinates and anisotropic thermal parameters. The final discrepancy factor $R = .026$ (Figs. 2 and 3).

Table 1. Cell constants of TNS.

Crystal A (hydrated)	Crystal B (anhydrous)
Parameter a	
12.1284 ± 0.0021 Å	6.1583 ± 0.0005 Å
Parameter b	
7.4774 ± 0.0016 Å	7.3793 ± 0.0007 Å
Parameter c	
19.9845 ± 0.0047 Å	17.4545 ± 0.0020 Å
Parameter α	
94.06 ± 0.02°	96.838 ± 0.010°
Parameter β	
98.90 ± 0.02°	95.820 ± 0.010°
Parameter γ	
93.07 ± 0.01°	92.667 ± 0.006°
Asymmetric unit	
2 TNS + $4H_2O$	1 TNS
Space group	
$P\bar{1}$	$P\bar{1}$

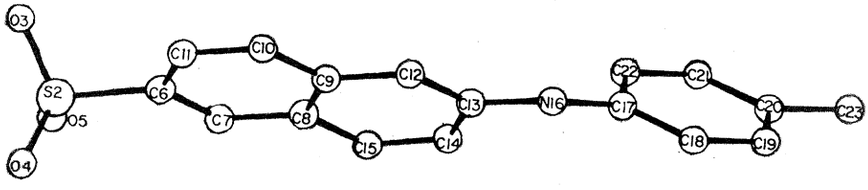

Fig. 2. Perspective drawing of the TNS molecule.

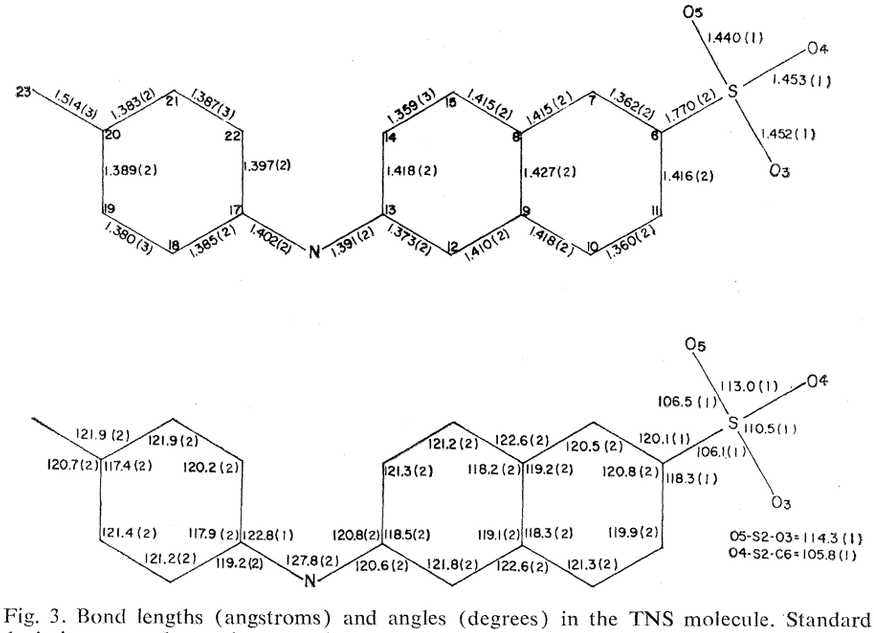

Fig. 3. Bond lengths (angstroms) and angles (degrees) in the TNS molecule. Standard deviations are shown in parentheses.

The compound TNS may be regarded as being made up of a planar naphthalene nucleus joined through N(16) to a planar tolyl group, the two planes making an angle of 49.6° to each other. There is ample evidence of electronic resonance over the whole molecule. The N atom has an approximately trigonal configuration; the sum of bond angles about N is 359.7° with the H atom 0.08 Å out of the plane of C(13)-N(16)-C(17), indicating sp^2 hybridization and a p^2 lone pair. The best plane through C(13)-N(16)-C(17)-H(16) makes angles of 25.4° and 27.7° with the naphthalene and tolyl planes, respectively; thus the overlap integral between each aromatic π system and the p^2 electrons of N is reduced only slightly from the value it would have if all orbitals were parallel. Bond lengths between N and C(13) and C(17) are 1.391 and 1.402 Å, significantly shorter than the length of the single bond between C(sp^2) and N(sp^2) of 1.470 Å (*5*). These data strongly suggest delocalization of the p electrons of N into an extended π electron system comprised of the N atom and benzene and naphthalene rings. Such a system contains 18 electrons and is in accordance with the Huckel $4n + 2$ rule for aromatic resonance stability. The C-N-C angle of 127.8° is larger than normal and may alleviate steric strain because of C-N bond shortening.

The emission shifts of fluorescent-probe compounds are generally interpreted in terms of Lippert's theory (*6*) involving dipole-dipole interactions during the lifetime of the excited state. If upon ultraviolet absorption the electronic delocalization stability of TNS is lessened, solvents with strong hydrogen bonding properties and appropriate steric size may lower the energy of the excited state by H···N(16) interaction. Similarly the geometry of protein binding sites to which TNS is attracted may affect the energy difference between ground and excited electronic states of the probe molecule and influence the probe's emission characteristics. It is therefore not entirely safe to assume that such probes measure only the polarity of the binding site, as has been suggested (*7*). The arrangement of water molecules about TNS in the hydrated crystals may be significant in supporting the speculation above.

ARTHUR CAMERMAN
L. H. JENSEN
Department of Biological Structure, University of Washington, Seattle 98105

References and Notes

1. G. M. Edelman and W. O. McClure, *Accounts Chem. Res.* **1**, 65 (1968).
2. W. O. McClure and G. M. Edelman, *Biochemistry* **5**, 1908 (1966).
3. ———, *ibid.* **6**, 567 (1967).
4. L. Stryer, *Science* **162**, 526 (1968).
5. A. Camerman, in preparation.
6. E. Lippert, *Z. Elektrochem.* **61**, 962 (1957).
7. D. C. Turner and L. Brand, *Biochemistry* **7**, 3381 (1968).

8. We thank Professor Martin Gouterman for aid in measuring the crystal fluorescence spectra. Supported by grant GM-13366 from the National Institutes of Health.

23 May 1969

Induction in vitro of Microtubular Crystals by Vinca Alkaloids

Abstract. *The addition of vinblastine or vincristine to solutions of pure microtubule protein or to supernatants from high-speed centrifugation of rabbit-brain homogenates results in the formation of a fine precipitate. Examination of this precipitate by electron microscopy reveals ordered structures with areas of ladder-like configuration.*

The vinca alkaloids, known for their metaphase-blocking antimitotic activity, induce a proliferation of 80- to 100-Å filaments (*1*) and the formation of microtubular crystals in the cytoplasm of various types of cells (*2*). The demonstration that a selective, quantitative precipitation of microtubule protein could be induced by vinblastine (*3*) suggested that similar filaments and crystals might be formed by the interaction of microtubule protein and the vinca alkaloids in vitro. We now report the formation of ordered structures from purified microtubule protein and supernatants obtained from high-speed centrifugation of rabbit-brain homogenates after the supernatants were incubated with vinblastine and vincristine.

Purified microtubule protein (colchicine-binding protein) was prepared from fresh pig brain (*4*). After reduction and alkylation the purified protein migrated as a single band on disc electrophoresis. Rabbit brains which had been freed of blood vessels and meninges were homogenized in 1.5 times the amount (weight to volume) of 1.15 percent KCl solution containing 3 m*M* $MgCl_2$ and 0.5 m*M* guanosine triphosphate (GTP) at *p*H 6.2 in a tissue grinder with a slowly rotating Teflon pestle at 4°C. The homogenate was centrifuged for 1 hour at 30,000*g* and the sediment was discarded. The GTP concentration was raised to 1 m*M*, and the *p*H was maintained at 6.2. The supernatant was then centrifuged at 100,000*g* for 1 hour. This high-speed supernatant was gently decanted and used for the experiments.

Portions of the supernatants and samples of the purified microtubule protein at concentrations of 1 to 2 mg/ml in 0.01*M* phosphate buffer containing 0.01*M* $MgCl_2$ and $10^{-4}M$ GTP at *p*H 6.5 were dialyzed against or incubated with $2 \times 10^{-4}M$ vinblastine or vincristine for 2 hours at 37°C. At the end of the incubation period a faint turbidity was noted in both the control and vinblastine-treated homogenates and also in the vinblastine-treated protein solution. The samples were then centrifuged at 30,000*g* for 30 minutes, and the sedimented pellets were fixed in 5 percent buffered glutaraldehyde at *p*H 6.5 followed by osmium tetroxide and embedded in Epon 812. Ultrathin sections were cut on the Reichert microtome, stained in uranyl acetate and lead citrate, and examined in a Siemens Elmiskop 1. The microscope was calibrated against a standard carbon-replica calibration grid.

Sections of the samples treated with vinca alkaloid revealed large areas of ordered structures with a ladder-like arrangement in the case of the pure protein preparations (Fig. 1), and more widely dispersed ladder-like structures in the rabbit-brain supernatant (Fig. 2). The ladders in both cases have "rungs" of approximately 80 Å in diameter (Fig. 3). The distance be-

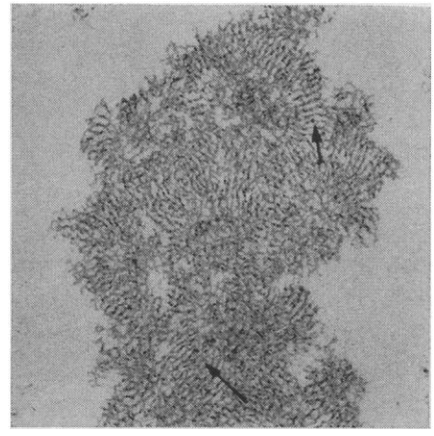

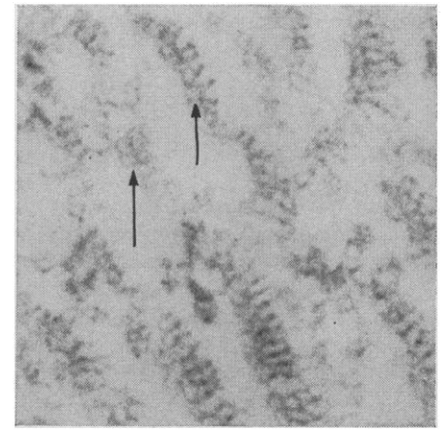

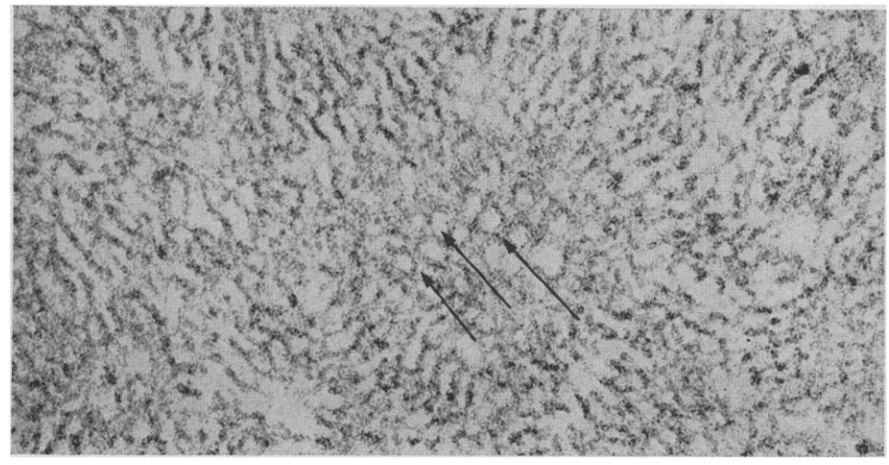

Fig. 1 (top left). Purified microtubule protein treated with $10^{-4}M$ vinblastine. Areas of ladder-like appearance (arrows) surround areas where circular profiles predominate (× 32,000). Fig. 2 (top right). Rabbit-brain supernatant treated with vinblastine. Dispersed "ladders" often appear to end in circular profiles (× 60,000). Fig. 3 (bottom). Purified microtubule protein treated with vinblastine showing detail of circular profiles (arrows) and of the 80-Å filamentous "rungs" arranged in an arciform pattern around them (× 115,000).